0023-6837/01/8105-725$03.00/0
LABORATORY INVESTIGATION
Copyright © 2001 by The United States and Canadian Academy of Pathology, Inc.
Vol. 81, No. 5, p. 725, 2001
Printed in U.S.A.

Metastatic Behavior of Human Breast Carcinomas Overexpressing the Bcl-x_L Gene: A Role in Dormancy and Organospecificity

Nuria Rubio, Laura España, Yolanda Fernández, Jerónimo Blanco, and Angels Sierra

Centre de Oncologia Molecular (NR, LE, YF, JB, AS), Institut de Recerca Oncológica, Hospital Duran i Reynals, Ciutat Sanitaria i Universitaria de Bellvitge, and Consejo Superior de Investigaciones Científicas (JB), Barcelona, Spain

SUMMARY: The ability of metastatic cells to survive antiapoptotic signals may contribute to the organospecific-spread patterns of clinical metastasis and dormancy. MDA-MB-435 breast cancer cells (435/Bcl-x_L), which overexpress the Bcl-x_L gene, were labeled with the luciferase gene and injected orthotopically into homozygous athymic Balb/c (nude) mice to study the metastatic behavior of the breast cancer cells. The overexpression of Bcl-x_L in tumors increased the overall metastatic burden in mice (bones, liver, kidneys, brain, lungs, and lymph nodes) in comparison with control tumors (435/Neo.luc) during the same time interval (ANOVA, $p = 0.005$). The principal differences after 110 days were found in bones, which had $1.5 \times 10^5 \pm 1.2 \times 10^5$ tumor cell equivalents ($p = 0.03$), and lymph nodes, which had $7.0 \times 10^6 \pm 6.0 \times 10^6$ tumor cell equivalents ($p = 0.08$). The analyses of light production by tissues at different times showed that cells from 435/Neo.luc and 435/Bcl-x_L.luc tumors were detectable in several organs by the second day after intramammary fat pad implantation. Although initially arriving at the target organs in similar numbers, 435/Bcl-x_L cells developed more metastases than 435/Neo cells, indicating that the Bcl-x_L gene might have a role in breast cancer dormancy, promoting survival of cells in metastatic foci. Thus, we suggest that overexpression of Bcl-x_L could counteract the proapoptotic signals in the microenvironment and favor the successful development of metastasis in specific organs. (*Lab Invest 2001, 81:725–734*).

Overexpression of the antiapoptotic proteins Bcl-2 and Bcl-x_L, associated with the loss of apoptosis in human breast-cancer tumors, may shift the balance between proapoptotic and antiapoptotic tendencies toward extending the lifespan of cells, thus having decisive consequences for tumor progression (Olopade et al, 1997; Rochaix et al, 1999; Sierra et al, 1998; Vakkala et al, 1999).

The expanding family of Bcl-2 genes includes death agonists and antagonists that share homology in as many as four amino acid regions, denoted as Bcl-2 homologies BH1, BH2, BH3, and BH4 (Minn et al, 1998). Proteins that inhibit apoptosis such as Bcl-2 or Bcl-x_L, exert their function by preventing the release of cytochrome c from the mitochondria to the cytosol, blocking both membrane hyperpolarization and mitochondrial swelling in response to several sets of stimuli (Kroemer et al, 1998; Vander Heiden et al, 1997). Overexpression of Bcl-2 or Bcl-x_L can confer resistance to most apoptotic stimuli, suggesting that these genes function at a central convergence point for many apoptotic pathways (Chao and Korsmeyer, 1998; Kroemer, 1997; Newton and Strasser, 1998). Moreover, Bcl-x_L interacts with Apaf-1 protein to inhibit the caspase activation that triggers apoptosis (Hu et al, 1998). Bcl-2 seems to exert its antiapoptotic activity partially through inhibiting the translocation of the proapoptotic protein Bax, and through the modification of cytosolic translocation factors (Nomura et al, 1999). However, gain of Bcl-2 function is dominant over loss of Bax function in regulating mammary epithelial cell survival in vivo (Schorr et al, 1999).

Molecular factors that influence tumor cell viability in situ, in the circulation, or in specific organs could influence metastasis (Shtivelman, 1997; Takaoka et al, 1997). Thus, the ability of a tumor cell to resist apoptotic signals may create favorable conditions for metastases development and, not surprisingly, highly metastatic cells tend to exhibit a greater survival ability and resistance to apoptosis than poorly metastatic ones (Glinsky and Glinsky, 1996). Indeed, Bcl-2 overexpression has been associated with an enhancement

Received February 6, 2001.
JB and AS contributed equally to the work. The doctoral fellow, Yolanda Fernández, was supported by Comissionat per a Universitats i Recerca de la Generalitat de Catalunya (CIRIT) and Merck Farma Química S.A. This study was supported by a grant from the Plan Nacional de Investigación Científica y Desarrollo Tecnológico (CICYT), SAF 97/0210; from the Ministerio de Sanidad y Consumo, FIS 99/0770; and from the Fundació D'Investigació Sant Pau.
Address reprint requests to: Dr. Angels Sierra, Centre de Oncologia Molecular, Institut de Recerca Oncològica, Autovia de Castelldefels, km 2.7, 08907 L' Hospitalet de Llobregat, Barcelona, Spain. E-mail: asierra@iro.es

of metastatic potential in human breast cancer cell lines inoculated in homozygous athymic Balb/c (nude) mice, because an increase in the survival of tumor cells ultimately promotes metastasis (Del Bufalo et al, 1997). Moreover, the inability of tumor cells to undergo apoptosis does not correlate with their tumorigenicity in nude mice, but it does correlate with their ability to survive in the lungs and form experimental metastases after intravenous injection (Nikiforov et al, 1997). Resistance to apoptosis could be an organo-selective determinant of metastatic behavior, because cells derived from a breast carcinoma brain metastasis are more resistant to apoptosis than lung metastatic cells from the same tumor, when exposed to growth factors from astrocytes (Sierra et al, 1997).

Recently, we analyzed several independent MDA-MB-435 breast cancer cell line clones that overexpress the Bcl-x_L gene and found that Bcl-x_L overexpression induces resistance to cytokine triggered apoptosis, increases cell survival in the circulation, and enhances anchorage-independent growth, rescuing metastatic cells from anoikis (Fernández et al, 2000). The contribution of antiapoptotic genes to metastases could result from the suppression of programmed cell death and extension of cell survival in aggressive environments. However, the specific role of antiapoptotic proteins in the dissemination from primary tumors to metastatic foci remains elusive, and it is uncertain at what stage cells may be rescued from apoptosis.

Although micrometastatic tumor cell aggregates can be identified by conventional histopathologic methods, individually disseminated carcinoma cells have generally resisted definitive cytologic identification. A luciferase-based method, devised for the direct measurement of metastatic dissemination kinetics in animal models, provides a rapid and highly sensitive assay for the detection of tumor cells lodged in target organs (De Wet et al, 1987; Rubio et al, 1998). We used this method to evaluate metastatic cells in different organs during 110 days after intramammary fat pad (IMFP) implantation.

The aim of this work was to elucidate how inhibition of apoptosis, caused by overexpression of the Bcl-x_L protein in breast cancer cells, could influence tumor dissemination and successful metastases development in specific organs. MDA-MB-435 breast cancer cells that overexpressed the Bcl-x_L gene were labeled with the luciferase gene (a tumor cell marker) and injected into the IMFP in nude Balb/c mice to study the metastatic behavior of the cancer cells.

Results

Light Production by 435/Neo.luc and 435/Bcl-x_L.luc Cells

The 435/Bcl-x_L cells overexpressed Bcl-x_L protein, as shown by Western blot comparative analyses of tumor cell lysates (Fig. 1A). Bcl-x_L expression was 2.8-fold higher in 435/Bcl-x_L cells than in the control clone 435/Neo.

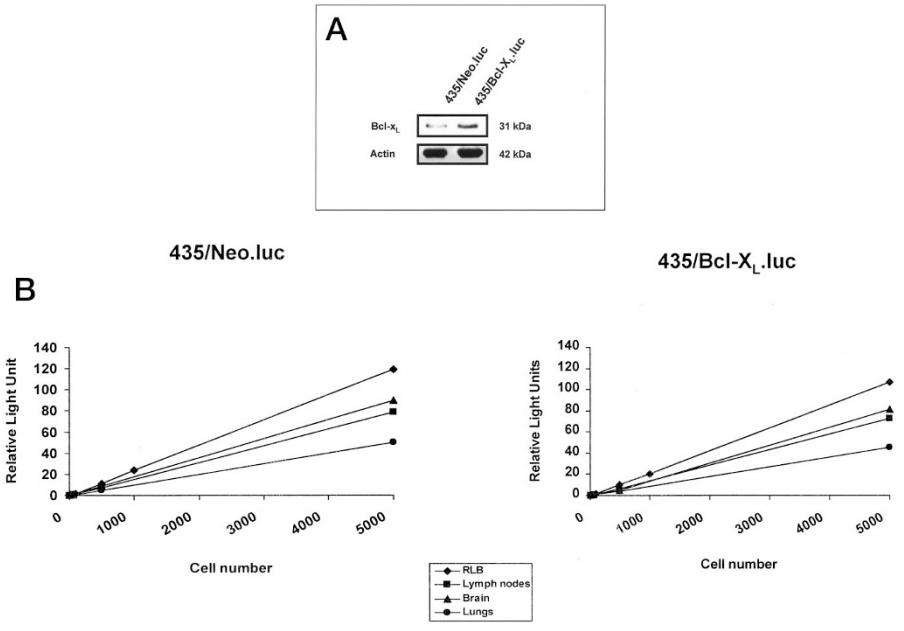

Figure 1.

A, Western blot analysis of Bcl-x_L expression in 435/Neo.luc and 435/Bcl-x_L.luc transfectants. Fifty micrograms of total protein from 435/Neo.luc and 435/Bcl-x_L.luc cells were fractionated by SDS-PAGE and transferred to a nitrocellulose membrane. The Bcl-x_L protein was detected as described, using a polyclonal antibody to Bcl-x_L and a peroxidase conjugated second antibody. Actin in the sample was used as an internal control detected with a monoclonal antibody to actin to monitor protein loads. The measured Bcl-x_L expression level was 2.8-times higher in 435/Bcl-x_L.luc than in 435/Neo.luc cells. B, Standard plots of light produced by 435 cells expressing the luciferase gene. Lysates derived from the indicated number of 435/Neo.luc or 435/Bcl-x_L.luc cells were mixed with a constant volume (20 μl) of either lysis buffer or clear lysate homogenate derived from the indicated tissues and directly measured for light production. Light emission is given in relative light units (RLU), proportional to photon numbers. Light production (*symbols*) and corresponding regression plots for each tissue homogenate and RLB are shown. Slopes of regression functions measure the amount of light produced by a single cell in 1 minute.

Luciferase-labeled tumor cells were generated by permanent transfection of 435/Neo and 435/Bcl-x_L cells with the plasmid pCEP4 containing the *Photinus pyralis* luciferase gene under transcriptional control of the cytomegalovirus promoter. The specific MDA-MB-435 clones chosen for luciferase tagging have metastatic behavior representative of control and Bcl-x_L–overexpressing cells (Fernández et al, 2000). Clones 435/Neo.luc and 435/Bcl-x_L.luc were selected for their high and similar light-producing capacity. In reporter lysis buffer, standard plots of light production versus number of cells were linear over a tested range of 0 to 5000 cells. The slopes of the regression plots, which are a measure of the amount of light produced during 1 minute by a single cell, corresponded to 0.023 and 0.021 relative light units (RLU)/cell for the 435/Neo.luc and 435/Bcl-x_L.luc cells, respectively.

The amount of light produced by known numbers of 435/Neo.luc and 435/Bcl-x_L.luc cells spiked into tissue homogenates was measured to determine the effect of tissue-specific components in light detection sensitivity. The slopes of the resulting standard curves measure the amount of light/cell per minute that can be detected effectively under the experimental conditions. These slopes were used to calculate the number of turner cell equivalents (TCEs) in the different target organs (Fig. 1B).

TCE Detection Sensitivity. TCE detection sensitivity for each organ was established as the number of TCEs necessary to generate an amount of RLU equivalent to twice the standard deviation of the background signal, measured using tissue homogenates lacking luminescent cells (Table 1). Sensitivity extremes for TCE detection varied from 1 to 8 TCEs per measurement, for muscle and liver, respectively. Taking the average mass of each organ into consideration, the minimum number of TCEs per organ that could be detected corresponded to 20 and 1053 TCEs, for lymph nodes and liver, respectively. Only values above the range of two standard deviations of the background noise are represented in the data.

Stability of Luciferase in Transfected Cells. Tumor cell explants from primary tumors, 45 days after inoculation, grew well in tissue culture in the presence of hygromycin and neomycin, producing 0.030 and 0.029 RLU/cell for 435/Neo.luc and 435/Bcl-x_L.luc, respectively, equivalent to those produced by the originally inoculated cells.

Bcl-x_L Increases Metastatic Activity of Breast Tumor Cells

The overexpression of Bcl-x_L increased the metastatic potential of MDA-MB-435 breast cancer cells when implanted IMFP (Fig. 2). Results from two-way ANOVA statistical analyses showed that the total number of TCEs detected in mice bearing the 435/Bcl-x_L.luc tumors was higher than that found in mice with the 435/Neo.luc tumors, regarding all organs analyzed (lungs, bones, liver, kidneys, brain, and lymph nodes). Results were based on data from days 45 and 110 after IMFP implantation ($p = 0.005$), with the removal of the primary tumor at day 45. Within the same group of mice, there was also a significant difference in metastatic burden ($p = 0.022$) between the two intervals, 45 and 110 days.

Visible macroscopic metastases in the lungs and lymph nodes developed in mice with 435/Bcl-x_L.luc tumors before the end of the experiment at day 110. In contrast, the 435/Neo.luc tumor-bearing mice had no detectable macroscopic metastases by the same time. These results were corroborated by histopatho-

Table 1. 435/Neo.luc and 435/Bcl-x_L.luc Cell Detection Sensitivity

		435/Neo.luc		435/Bcl-X_L.luc	
	Background[a]	Sensitivity[b]	Number of detectable TCEs per organ	Sensitivity[b]	Number of detectable TCEs per organ
Brain	0.023 ± 0.026	2.99	114	3.36	128
Lymph nodes	0.017 ± 0.029	3.68	20	3.92	22
Ribs	0.043 ± 0.028	4.42	367	5.15	401
Ovaries	0.030 ± 0.033	5.53	39	6.04	43
Muscle	0.040 ± 0.002	0.41	28	0.41	28
Lungs	0.029 ± 0.026	5.21	74	5.79	83
Liver	0.016 ± 0.028	6.28	819	8.08	1053
Breast	0.043 ± 0.037	4.69	27	5.78	34
Vertebral column	0.014 ± 0.024	3.23	393	3.46	421
Mediastinal	0.036 ± 0.032	4.95	37	5.36	40
Kidneys	0.017 ± 0.030	6.11	201	6.79	223
Femur	0.036 ± 0.032	7.13	56	7.13	57
Spleen	0.031 ± 0.028	7.04	81	8.04	93

TCEs, tumor cell equivalents.

[a] Background from counting instrument plus tissue homogenate in the absence of light-producing cells (expressed as relative light units).

[b] Number of cells equivalent to 2 times the standard deviation of background.

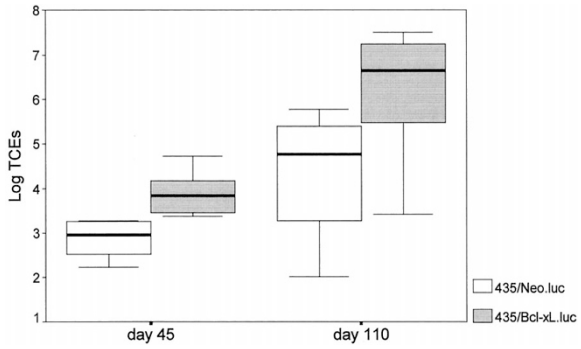

Figure 2.

Pock plot graphic histograms showing the logarithm of the total number of tumor cell equivalents (Log TCEs) found in all of the analyzed organs, at days 45 and 110 after IMFP implantation, for 435/Neo.luc and 435/Bcl-x_L.luc cells. The median and interquartile ranges of each group are indicated. The number of metastatic cells was different between the two groups of mice (ANOVA, $p = 0.005$), and within the same group of mice at the two different times (ANOVA, $p = 0.022$).

logic analyses of consecutive paraffin-embedded tissue sections (data not shown).

Cell Dissemination and Metastatic Growth in Different Organs

Table 2 describes the distribution of TCEs detected in several organs. The most affected organs after 45 days for 435/Bcl-x_L.luc mice were the lungs ($4.5 \times 10^3 \pm 2.4 \times 10^3$ TCEs), lymph nodes ($2.6 \times 10^2 \pm 1 \times 10^2$ TCEs), and bones ($1.1 \times 10^4 \pm 9.5 \times 10^3$ TCEs). At the end of the experiment (110 days), lymph nodes were the most important metastatic target, containing $7.0 \times 10^6 \pm 6.0 \times 10^6$ TCEs, followed by lungs with $3.5 \times 10^6 \pm 3.4 \times 10^6$ TCEs, bones at $1.5 \times 10^5 \pm 1.2 \times 10^5$ TCEs, and brain contained $1 \times 10^3 \pm 0.9 \times 10^3$ TCEs.

For the 435/Neo.luc tumors, lungs were the only organs significantly affected at days 45 and 110, with a total of $4.4 \times 10^2 \pm 1.7 \times 10^2$ TCEs and $1.8 \times 10^5 \pm 1.4 \times 10^5$ TCEs, respectively. At day 110, the other organs had less than 100 TCEs.

By the end of the experiment there were significant differences in the metastatic burden to bones ($p = 0.03$) and lymph nodes ($p = 0.08$) between Bcl-x_L and control tumors. However, for lungs, also a typical target organ for breast carcinomas, the metastatic burdens from both Bcl-x_L and control tumors were similar ($p = 0.8$).

The analyses of TCEs at different time intervals showed that cells from 435/Neo.luc and 435/Bcl-x_L.luc tumors were detectable in several organs (such as lungs, bones, lymph nodes, and some viscera) 2 days after IMFP implantation (Fig. 3). The number of TCEs increased in lungs after 30 days, and progressed until day 110 in both groups of mice. In the 435/Bcl-x_L.luc mice, TCEs also increased in bones and in lymph nodes. In viscera (liver, kidneys, brain, and ovaries), the total number of TCEs was similar for the two groups of mice studied, remained low throughout the experiment, and no discrete tumors were found at any time.

Tumorigenicity of 435/Neo.luc and 435/Bcl-x_L.luc Cells

The tumor incidence was 100% in the two groups of mice. Tumors appeared 2 weeks after cells were injected IMFP, and were excised after 45 and 100 days.

Tumor volume was calculated using the formula: Volume (mm^3) = $L \times W^2/2$, where L and W are the major and minor diameters in millimeters, respectively. Tumorigenic differences were observed between 435/Neo.luc and 435/Bcl-x_L.luc cells (Fig. 4). The mean tumor volumes were: 80.7 ± 50.8 mm^3 and 223.0 ± 96.0 mm^3 at day 45; and 132.4 ± 65.4 mm^3 and 716.4 ± 615.5 mm^3 at day 100, for 435/Neo.luc and 435/Bcl-x_L.luc mice, respectively.

We also measured the number of 435/Neo.luc and 435/Bcl-x_L.luc cells in the tumors by assessing light production. The ratio of light producing TCEs/mg of tumor remained similar for both types of tumors throughout the experiment (Table 3).

Relation between Primary Tumor Size and Metastatic Activity

To evaluate the influence of the primary tumor in metastatic activity, we compared the ratio of TCEs in target organ to TCEs in tumor (metastases ratio) from days 2 through 100, for both Bcl-x_L.luc and control tumors (Fig. 5).

At the second day after IMFP, the metastatic ratio was similar for both the Bcl-x_L.luc and control mice. From day 15 on, this ratio was higher for the Bcl-x_L.luc than for the control mice, although both groups of mice showed a steady and time-related increase in the metastasis ratio.

We also analyzed the influence of continuous primary tumor growth in metastatic activity. For this purpose, we compared metastasis development between the group of mice that had their primary tumors remove at day 45 with a second group of mice, in which tumors were allowed to remain until day 100 (Fig. 6). There was a significant positive effect of tumor presence on metastases growth past day 45 only for viscera (in mice with both types of tumor) and bones (in the 435/Neo.luc mice). However, for the rest of organs and for mice with both types of tumor, removal of the primary tumors at day 45 favored metastatic development.

Discussion

In human breast carcinomas, the overexpression of the antiapoptotic Bcl-x_L protein increases metastatic potential. Recently, we reported that breast cancer cells overexpressing Bcl-x_L acquire resistance against cytokines and override apoptosis, have enhanced anchorage-independent growth caused by a modified interaction with the extracellular matrix, and have increased cell survival in the circulation (Fernández et al, 2000). The present results show that metastatic tumor cells arrive at many organs soon after the start of the experiment. However, metastasis growth was differentially af-

Table 2. Metastatic Activity of Breast Tumor Cells Expressed as TCEs in Different Organs

	Day 45			Day 110		
	435/Neo.luc mean ± SE (No. affected/No. tested)	435/Bcl-X_L.luc mean ± SE (No. affected/No. tested)	*p*	435/Neo.luc mean ± SE (No. affected/No. tested)	435/Bcl-X_L.luc mean ± SE (No. affected/No. tested)	*p*
Lungs	$4.4 \times 10^2 \pm 1.7 \times 10^2$ (4/5)	$4.5 \times 10^3 \pm 2.4 \times 10^3$ (5/5)	0.05	$1.8 \times 10^5 \pm 1.4 \times 10^5$ (3/4)	$3.5 \times 10^6 \pm 3.4 \times 10^6$ (5/5)	0.80
Lymph nodes[a]	7 ± 4 (3/5)	$2.6 \times 10^2 \pm 1 \times 10^2$ (4/5)	0.06	85 ± 27 (4/4)	$7 \times 10^6 \pm 6 \times 10^6$ (5/5)	0.08
Bones[b]	$3.9 \times 10^2 \pm 1.8 \times 10^2$ (4/5)	$1.1 \times 10^4 \pm 9.5 \times 10^3$ (3/5)	0.91	70 ± 57 (4/4)	$1.5 \times 10^5 \pm 1.2 \times 10^5$ (5/5)	0.03
Liver	23 ± 23 (1/5)	28 ± 28 (1/5)	0.88	0	$1.6 \times 10^2 \pm 1 \times 10^2$ (2/5)	0.18
Kidneys	6 ± 6 (1/5)	9 ± 9 (1/5)	0.88	0	63 ± 43 (2/5)	0.18
Brain	0	0	1	31 ± 30 (2/4)	$1 \times 10^3 \pm 0.9 \times 10^3$ (5/5)	0.14
Contralateral breast	$1 \times 10^2 \pm 1 \times 10^2$ (2/5)	69 ± 32 (4/5)	0.39	2 ± 2 (1/4)	16 ± 14 (3/5)	0.61
Ovaries	49 ± 41 (2/5)	0	0.05	3 ± 2 (2/4)	27 ± 14 (4/5)	0.08
TOTAL	$1.0 \times 10^3 \pm 3.6 \times 10^2$ (5/5)	$1.6 \times 10^4 \pm 0.9 \times 10^4$ (5/5)	0.01	$1.8 \times 10^5 \pm 1.4 \times 10^5$ (4/4)	$1.1 \times 10^7 \pm 6 \times 10^6$ (5/5)	0.14

[a] Lymph nodes include mediastenial, cervical, axillar, brachial, and inguinal nodes.
[b] Bones include ribs, vertebral column, and femur.

fected by the physiologic environment of target organs and by the capacity of Bcl-x_L–overexpressing cells to overcome death signals.

Time-lapse videomicroscopic observation of melanoma cells injected into the circulation documented the failure of a solitary cells to initiate growth in metastatic sites and the need for a permissive environment to sustain growth (Luzzi et al, 1998).

Cells from 435/Bcl-x_L.luc tumors seeded early in peripheral lymph nodes, bones, brain, and lungs, but macroscopic metastases appeared only in lymph nodes and lungs, also typical sites for human breast cancer metastases (Fernández et al, 2000; Pantel et al, 1999). Both control and Bcl-x_L tumors showed no statistically significant difference in their capacity for lung metastasis, typical of breast carcinomas. However, there was a clear and statistically significant difference in their capacity to metastasize to bones and lymph nodes.

Thus, we suggest that Bcl-x_L overexpression in breast carcinomas could counteract proapoptotic signals and favor development of metastases, helping to explain the clinically observed metastasis organospecificity. However, the role of Bcl-x_L in determining tumor cell dissemination kinetics from primary tumors to metastatic foci remains elusive, because we did not find organ-related differences in their number distribution on arrival. "Tumor dormancy" describes a prolonged quiescent state, during which metastasis progression is not clinically detected (Yefenof et al, 1993).

Metastasis is a biologic process that is a part of breast cancer progression. Metastatic cells may be present after surgery but remain dormant for several reasons. They may be unable to induce angiogenesis or to change the balance between other growth-inducing or growth-inhibiting factors in the tumor microenvironment, which may also determine the length of the period between dissemination and the appearance of clinically manifest metastases (Hart, 1999; Karrison et al, 1999).

Holmgren et al (1995) suggest that dormancy could be the consequence of opposing tumor cell proliferative tendencies by antiangiogenic factors that indirectly promote apoptosis, as demonstrated in Lewis lung carcinoma. In a murine B-cell leukemia system, dormancy was described as the result of an active antiproliferative mechanism operating via anti-idiotype reactivity (Riethmüller et al, 1999). 435/Neo.luc and 435/Bcl-x_L.luc cells arrived at target organs in similar numbers. However, in some organs, 435/Neo cells failed to develop metastases whereas 435/Bcl-x_L metastases did develop, indicating that Bcl-x_L might displace the balance between death and proliferation tendencies toward growth, overcoming dormancy.

We propose that overexpression of the antiapoptotic protein Bcl-x_L promotes escape from dormancy in breast cancer cells by displacing the death/proliferation equilibrium in the direction of

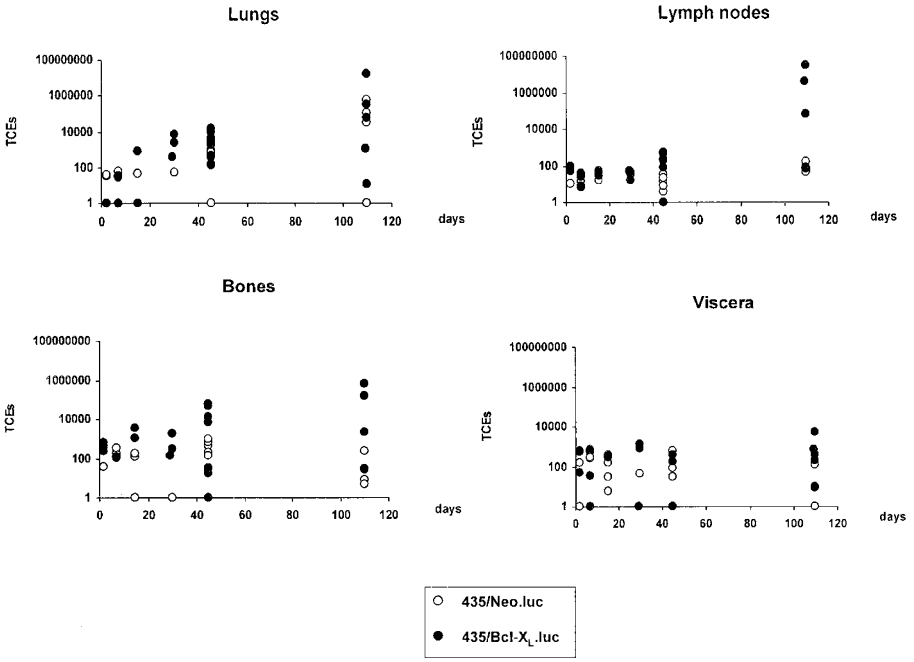

Figure 3.

Accumulation of 435/Bcl-x_L.luc and 435/Neo.luc cells as a function of time after IMFP implantation in the different organ sets. Data points show, for each of the mice in the group, the sum of TCEs found in lungs, lymph nodes (including mediastinal, cervical, axillar, brachial, and inguinal), bones (including ribs, vertebral column, and femur) and viscera (including liver, kidneys, ovaries, and brain). The number of circles represents the number of mice in each group. *Empty circles*, 435/Neo.luc; *filled circles*, 435/Bcl-x_L.luc.

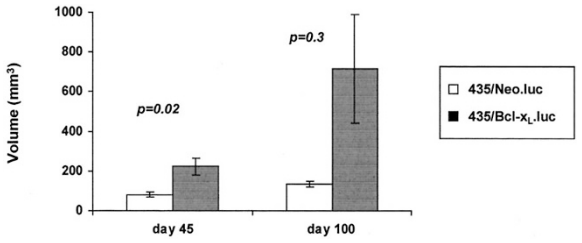

Figure 4.

Histogram showing tumorigenicity of 435/Bcl-x_L.luc and 435/Neo.luc cells at 45 and 100 days after IMFP implantation. 1×10^6 435/Bcl-x_L.luc (*black bars*) or 435/Neo.luc cells (*white bars*), were IMFP implanted and the tumor volumes calculated at the indicated times using the formula volume (mm^3) = $L \times W^2/2$, where L and W are the major and minor diameters in millimeters, respectively. Standard deviation bars and *p* significance values are indicated in the figure (Mann-Whitney test).

enhanced survival and adaptation to a new microenvironment.

Our results show that tumor cells disseminated early after IMFP implantation and did not require extensive tumor growth to enter the vascular and lymphatic systems, significantly decreasing the time available to perform in vivo diagnostic analyses of metastatic potential. These results suggest that, in clinical situations, systemic disease may be prevalent earlier than usually suspected for these tumors. Furthermore, systemic disease may not manifest until the interaction of the tumor cells with the microenvironment favors proliferation. Mice in which the primary tumors were removed after 45 days did not show a lower metastatic success compared with mice bearing tumors throughout the 100 days of the experiment, indicating that the observed metastasis grew from early arriving tumor cells. Moreover, the continuous presence of the primary tumor generally resulted in a lower metastatic burden. This fact suggests the existence of antiproliferative factors (possibly antiangiogenic) that control metastatic development secreted by the primary tumors (Holmgren et al, 1995; O'Reilly et al, 1994).

Orthotopic implantation is becoming widely accepted as an accurate tumor model. There is evidence from various tumor tissues that orthotopic implantation can significantly increase the metastatic capacity of some xenografts growing in nude mice (Burger, 2000; Clarke and Dickson, 1997). Thus, it is desirable to develop models that parallel metastatic spread in a disease specific fashion even more stringently; possibly using immunocompetent animals.

The molecular mechanisms that enable individual cells to escape from the tumor, ie, to migrate and survive, remain essentially unknown. However, they likely represent independent activities that, having otherwise deleterious effects in normal cells, may coincide in tumor cells to promote metastasis (McCawley and Matrisian, 2000; Wells, 2000). We suggest that overexpressed Bcl-x_L is one such activity that, by providing a mechanism for tumor cell survival in new and nonpermissive environments, contributes to the organospecific pattern of clinical metastatic spread.

Our results emphasize the need for further study of the early stages of metastatic dissemination during the

Table 3. Stability of Light Production Capacity during Tumor Growth: Light Producing TCEs/mg of Tumor Tissue

435/Neo.luc TCEs/mg (mean ± SE)			435/Bcl-X_L.luc TCEs/mg (mean ± SE)		
Day 45	Day 100	*p*	Day 45	Day 100	*p*
87193 ± 8253	103854±49253	0.74	104173±9797	108464±16127	0.75

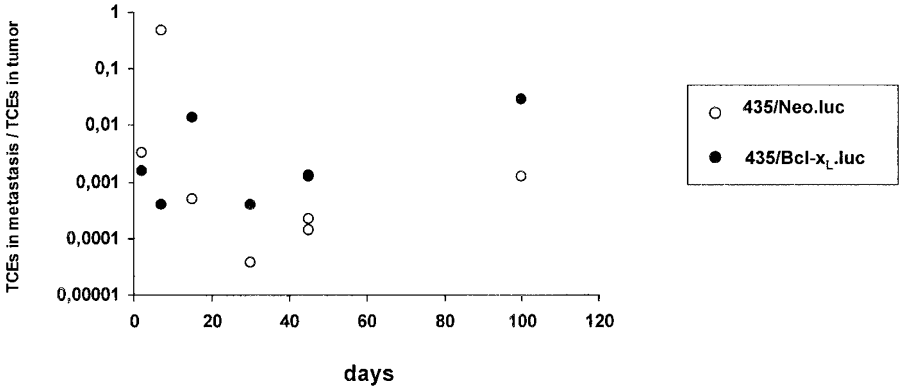

Figure 5.

Evolution of the total metastatic burden relative to tumor size versus time of tumor growth. The graph shows the ratio of total metastatic TCEs in all organs to total TCEs in the primary tumor versus time after IMFP implantation, for 435/Neo.luc (*empty circles*) and 435/Bcl-x_L.luc cells (*filled circles*). Data points represent the average ratio for each group of mice.

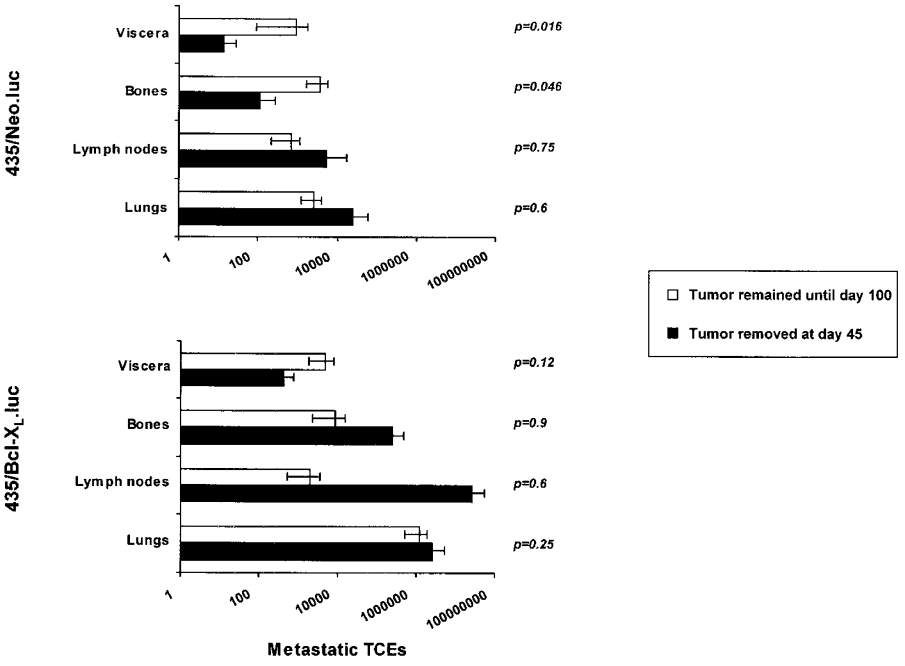

Figure 6.

Dependence of metastatic burden, in each set of organs, versus tumor presence. The histograms show the total number of metastatic TCEs in each organ set, from mice with (*white bars*) or without (*black bars*) primary tumors at day 100, for 435/Neo.luc and 435/Bcl-x_L.luc tumors. The organ sets were lungs, lymph nodes (cervical, axillar, brachial, and inguinal), bones (ribs, vertebral column, and femur), and viscera (liver, kidneys, and ovaries). Standard deviation bars and *p* significance values are indicated in the figure (Mann-Whitney test).

natural history of human breast cancer to optimize prognosis and treatment. Moreover, antiapoptotic genes seem to be attractive targets for gene-directed therapy and understanding the role of antiapoptotic genes in metastasis dormancy may offer insight for the design of new therapeutic strategies.

Material and Methods

Human Breast Carcinoma Cell Cultures and Transfections

MDA-MB-435 cell cultures were maintained in a 1:1 (v/v) mixture of DMEM and Ham's F12 medium (DMEM/F12) supplemented with 10% fetal bovine

serum, 2 mM L-glutamine, and 1 mM Pyruvate in 5% CO_2 at 37° C in a humidified incubator. MDA-MB-435 cells were transfected with the eukaryotic expression vectors PSFFVneo Bcl-x_L or PSFFVneo (kindly provided by Dr. J. L. Fernández-Luna, Unidad de Genetica Molecular, University of Santander, Santander, Spain), containing the Bcl-x_L and neomycin resistance gene coding regions, respectively, under control of the cytomegalovirus promoter. Clones MDA-MB-435/Neo (435/Neo) and MDA-MB-435/Bcl-x_L (435/Bcl-x_L), selected for these experiments, were previously analyzed in vivo and in vitro to avoid the possibility of clonal variations (Fernández et al, 2000).

435/Neo and 435/Bcl-x_L clones had the characteristic metastatic behavior of previously described control and Bcl-x_L overexpressing clones, respectively (Fernández et al, 2000). Both clones were transfected with the luciferase gene (Rubio and Blanco, 1996) using the pCEP4 expression vector (Invitrogen, San Diego, California) containing the firefly (*Photinus pyralis*) luciferase and hygromycin-resistance gene-coding regions and cloned, as described (Rubio et al, 2000).

Detection of Bcl-x_L Expression by Western-Blot Analysis

Cells from exponential cultures were lysed in 200 μl of buffer (50 mM Tris, 150 mM NaCl, 0.1% SDS, 1% NP-40, 0.5% sodium deoxycholate). Lysate volumes for each cell line containing 50 μg of protein, as determined by BCA protein assay (Pierce, Rockford, Illinois), were analyzed by SDS-PAGE, and the fractionated proteins transferred to nitrocellulose membranes (Hybond ECL; Amersham Corporation, Arlington Heights, Illinois). Nonspecific protein-binding sites in the membranes were blocked by a 5% solution of nonfat dry milk in PBS. For antigen detection, the membranes were incubated with a polyclonal rabbit antibody specific for human Bcl-x proteins at a 1:1000 dilution (Santa Cruz Biotechnology, Santa Cruz, California). A peroxidase-conjugated secondary antibody (Amersham) was used to detect specific reactivity. The ECL chemiluminescence reaction (Amersham) was used to visualize immunoreactive bands on Hyperfilm MP (Amersham). Molecular weights (MW) were established using prestained MW calibration markers (Bio-Rad Laboratories S.A., Madrid, Spain). Equal loading of protein samples was monitored using actin as an internal standard detected with a monoclonal antibody to human actin (Sigma, St. Louis, Missouri). X-ray films were scanned and analyzed using Molecular Analyst Software (Bio Rad, Richmond, California).

Luciferase Assay

Luciferase activity in extracts of cells or tissues was measured by chemiluminescence using the standard luciferase assay kit (Promega Corporation, Madison, Wisconsin). Production of light was measured using a Turner Desings luminometer, model TD 20/20, after addition of 100 μl of luciferase assay reagent (Promega Corporation) to a 20 μl aliquot of cell lysate or tissue homogenate (Rubio et al, 2000). Light detector measurements were expressed in RLU.

Light Detection Standard Curves. Standard curves to evaluate light detection linearity and sensitivity in tissue extracts were generated by measuring light production in a mixture consisting of lysate from a predetermined number of MDA-MB-435.luc cells, ranging from 0 to 5000 cells, in reporter lysis buffer (RLB) and 20 μl of clear tissue homogenate, prepared as described below, from mice not exposed to luminescent cells. Another standard control reference curve was generated with RLB substituted for the tissue homogenate.

Counting of Tumor Cell Equivalents and Detection Sensitivity. To calculate the number of 435.luc TCEs present in mice tissues, the corresponding background signal was subtracted from the RLU produced by a 20 μl aliquot of tissue homogenate, and the resulting number was divided by the slope of the corresponding tissue homogenate "light-detection standard curve." Tissue homogenates in which the luciferase activity of a 20-μl aliquot exceeded the detector range capacity were adjusted to the counter range by dilution with RLB. Assay sensitivity was defined as the number of TCEs required to generate a quantity of light equivalent to two standard deviations of the background signal. Only TCE values above the assay sensitivity limit were included in the data.

Cell and Tissue Homogenates. Cell lysates were prepared by performing one freeze-thaw cycle in RLB (Promega Corporation). Whole organ and tissue extracts were prepared by mechanical homogenization of tissues in RLB at a 1:1 ratio (w/v), using an Ultra-Turrax T-25 tissue homogenizer (Janke and Kunkel, Staufen, Germany) and centrifugation at 25,000 $\times$ g for 45 minutes at 4° C to remove insoluble particles. For lymph nodes, tissue was homogenized in the presence of 10% bovine serum albumin to protect against proteases.

Generation of Primary Tumors and Metastases in Nude Balb/c Mice. Six-to-seven-week-old athymic nude Balb/c female mice were used to grow tumors IMFP (Zhang et al, 1991). Mice were purchased from IFFA-CREDO (L'Arbresle, France) and maintained in a specific pathogen-free environment throughout the experiment. A suspension of 1×10^6 cells in 0.05 ml of serum-free medium was injected IMFP. Randomly chosen animals were killed by ether anesthesia and examined for metastases by measuring light production, starting at day 2 after IMFP implantation until day 110. Tumors were removed at day 45 in all animals, except for one group, in which tumors were not removed until day 100. Necropsies were performed and primary tumors and organs harvested and weighed. Metastatic involvement was independently monitored by analysis of haematoxylin and eosin-stained paraffin sections.

Analysis of Tumor Data

Statistical analysis of data was performed using Statistical Package of the Social Sciences (SPSS) for

Windows. The estimated number of cells from light measurements were logarithm transformed (log) to reduce dispersion. Two-way ANOVA was used to compare means according to the group of mice (mice with 435/Neo.luc tumors and mice with 435/Bcl-x_L.luc tumors) and point in time of evaluation (45 or 110 days). The nonparametric Mann-Whitney *U* test was also used for two-group comparisons. Two-tiled *p*-values smaller than 0.05 were regarded as statistically significant. Microsoft Excel was used for the graphic representation of data.

Acknowledgement

We thank Victor Moreno from the Servei d'Epidemiologia i Registre del Càncer Institut Català d'Oncologia, Ciutat Sanitària i Universitària de Bellvitge, Barcelona, Spain, for his advice in the statistical analyses of data.

References

Burger MM (2000). UICC study group on basic and clinical cancer research: Animal models for the natural history of cancer. Int J Cancer 85:303–305.

Chao DT and Korsmeyer SJ (1998). Bcl-2 family: Regulators of cell death. Annu Rev Immunol 16:395–419.

Clarke R and Dickson RB (1997). Animal models of tumor onset, growth, and metastasis. In: Bertino JR, editor. Encyclopedia of Cancer, vol 1. San Diego: Academic Press, 10–21.

Del Bufalo D, Biroccio A, Leonetti C, and Zupi G (1997). Bcl-2 overexpression enhances the metastatic potential of a human breast cancer line. FASEB J 11:947–953.

De Wet JR, Wood KV, DeLuca M, Helinski DR, and Subramani S (1987). Firefly luciferase gene: Structure and expression in mammalian cells. Mol Cell Biol 7:725–737.

Fernández Y, España L, Mañas S, Fabra A, and Sierra A (2000). Bcl-x_L promotes metastasis of breast cancer cells by induction of cytokines resistance. Cell Death Differ 7:350–359.

Glinsky GV and Glinsky VV (1996). Apoptosis and metastasis: A superior resistance of metastatic cancer cells to programmed cell death. Cancer Lett 101:43–51.

Hart IR (1999). Perspective: Tumour spread: The problems of latency. J Pathol 187:91–94.

Holmgren L, O'Reilly MS, and Folkman J (1995). Dormancy of micrometastases: Balanced proliferation and apoptosis in the presence of angiogenesis suppression. Nat Med 1:149–153.

Hu Y, Benedict MA, Wu D, Inohara N, and Núñez G (1998). Bcl-x_L interacts with Apaf-1 and inhibits Apaf-1-dependent caspase-9 activation. Proc Natl Acad Sci USA 95:4386–4391.

Karrison TG, Ferguson DJ, and Meier P (1999). Dormancy of mammary carcinoma after mastectomy. J Natl Cancer Inst 91:80–85.

Kroemer G (1997). The proto-oncogene Bcl-2 and its role in regulating apoptosis. Nat Med 3:614–620.

Kroemer G, Dallaporta B, and Resche-Rigon M (1998). The mitochondrial death/life regulator in apoptosis and necrosis. Annu Rev Physiol 60:619–642.

Luzzi KJ, MacDonald IC, Schmidt EE, Kerkvliet N, Morris VL, Chambers AF, and Groom AC (1998). Multistep nature of metastatic inefficiency. Dormancy of solitary cells after successful extravasation and limited survival of early micrometastases. Am J Pathol 153:865–873.

McCawley LJ and Matrisian LM (2000). Matrix metalloproteinases: Multifunctional contributors to tumor progression. Mol Med Today 6:149–156.

Minn AJ, Swain RE, Ma A, and Thompson CB (1998). Recent progress on the regulation of apoptosis by Bcl-2 family members. Adv Immunol 70:245–279.

Newton K and Strasser A (1998). The Bcl-2 family and cell death regulation. Curr Opin Genet Dev 8:68–75.

Nikiforov MA, Kwek SSS, Mehta R, Artwohl JE, Lowe SW, Gupta TD, Deichman GI, and Gudkov AV (1997). Suppression of apoptosis by bcl-2 does not prevent p53-mediated control of experimental metastasis and anchorage dependence. Oncogene 15:3007–3012.

Nomura M, Shimizu S, Ito T, Narita M, Matsuda H, and Tsujimoto Y (1999). Apoptotic cytosol facilitates Bax translocation to mitochondria that involves cytosolic factor regulated by Bcl-2. Cancer Res 59:5542–5548.

Olopade OI, Adeyanju MO, Safa AR, Hagos F, Mick R, Thompson CB, and Recant WM (1997). Overexpression of Bcl-x protein in primary breast cancer is associated with high tumor grade and nodal metastases. Cancer J Sci Am 4:230–237.

O'Reilly MS, Holmgren L, Shing Y, Chen C, Rosenthal RA, Moses M, Lane WS, Cao Y, Sage EH, and Folkman J (1994). Angiostatin: A novel angiogenesis inhibitor that mediates the suppression of metastases by a Lewis lung carcinoma. Cell 79:315–328.

Pantel K, Cote RJ, and Fodstad O (1999). Detection and clinical importance of micrometastatic disease. J Natl Cancer Inst 91:1113–1124.

Riethmüller G, Klein CA, and Pantel K (1999). Hunting down the seminal cells of clinical metastases. Immunol Today 20:294–296.

Rochaix P, Krajewski S, Reed JC, Bonnet F, Voigt J-J, and Brousset, P (1999). In vivo patterns of Bcl-2 family protein expression in breast carcinomas in relation to apoptosis. J Pathol 187:410–415.

Rubio N and Blanco J (1996). Simultaneous selection and cloning of transfected eukaryotic cells. Biotechniques 21: 622–624.

Rubio N, Villacampa MM, and Blanco J (1998). Traffic to lymph nodes of PC-3 prostate tumor cells in nude mice visualized using the luciferase gene as a tumor cell marker. Lab Invest 78:1315–1325.

Rubio N, Villacampa MM, El Hilali N, and Blanco J (2000). Metastatic burden in nude mice organs measured using prostate tumor PC-3 cells expressing the luciferase gene as a quantifiable tumor cell marker. Prostate 44:133–143.

Schorr K, Li M, Bar-Peled U, Lewis A, Heredia A, Lewis B, Knudson CM, Korsmeyer SJ, Jäger R, Weiher H, and Furth PA (1999). Gain of Bcl-2 is more potent than Bax loss in

regulating mammary epithelial cell survival in vivo. Cancer Res 59:2541–2545.

Shtivelman E (1997). A link between metastasis and resistance to apoptosis of variant small cell lung carcinoma. Oncogene 14:2167–2173.

Sierra A, Castellsagué X, Escobedo A, Lloveras B, Moreno A, and Fabra A (1998). Expression of death-related genes and their relationship with loss of apoptosis in T_1 ductal breast carcinomas. Int J Cancer 79:103–110.

Sierra A, Price JE, García-Ramirez M, Méndez O, López L, and Fabra A (1997). Astrocyte-derived cytokines contribute to the metastatic brain specificity of breast cancer cells. Lab Invest 77:357–368.

Takaoka A, Adachi M, Okuda H, Sato S, Yawata A, Hinoda Y, Takayama S, Reed JC, and Imai K (1997). Anti-cell death activity promotes pulmonary metastasis of melanoma cells. Oncogene 14:2971–2977.

Vakkala M, Lähteenmäki K, Raunio H, Pääkkö P, and Soini Y (1999). Apoptosis during breast carcinoma progression. Clin Cancer Res 5:319–324.

Vander Heiden MG, Chandel NS, Williamson EK, Schumacker PT, and Thompson CB (1997). Bcl-x_L regulates the membrane potential and volume homeostasis of mitochondria. Cell 91:627–637.

Wells A (2000). Tumor invasion: Role of growth factor-induced cell motility. Adv Cancer Res 78:31–101.

Yefenof E, Picker LJ, Scheuermann RH, Tucker T F, Vitetta ES, and Uhr JW (1993). Cancer dormancy: Isolation and characterization of dormant lymphoma cells. Proc Natl Acad Sci USA 90:1829–1833.

Zhang RD, Fidler IJ, and Price JE (1991). Relative malignant potential of human breast carcinoma cell lines established from pleural effusions and a brain metastasis. Invasion Metastasis 11:204–215.